



## Non-invasive caffeinated-nanovesicles as adipocytes-targeted therapy for cellulite and localized fats

Lobna M. Khalil<sup>a</sup>, Wessam M. El-Refaie<sup>b</sup>, Yosra S.R. Elnaggar<sup>a,b</sup>, Hamdy Abdelkader<sup>c,\*</sup>, Adel Al Fatease<sup>c</sup>, Ossama Y. Abdallah<sup>a</sup>

<sup>a</sup> Department of Pharmaceutics, Faculty of Pharmacy, Alexandria University, Alexandria, Egypt

<sup>b</sup> Department of Pharmaceutics and Pharmaceutical Technology, Faculty of Pharmacy, Pharos University in Alexandria, Alexandria, Egypt

<sup>c</sup> Department of Pharmaceutics, College of Pharmacy, King Khalid University, Abha 62223, Saudi Arabia

### ARTICLE INFO

#### Keywords:

Targeting  
Nanotechnology  
Adenosine receptors  
Topical drug delivery  
Caffeine

### ABSTRACT

Caffeine (CAF) is a non-selective adenosine A1 receptor antagonist which predominates in fat cells. When CAF binds to adenosine receptors, it increases cyclic adenosine monophosphate; inhibiting adipogenesis and inducing fat lipolysis. Resveratrol (RSV) is an antioxidant polyphenol possessing different anti-obesity mechanisms. Topical application of both hydrophilic CAF and lipophilic RSV is limited.

This study aimed to develop novel caffeinated-resveratrol bilosomes (CRB) and caffeine-bilosomes (CB) that could non-invasively target and deposit in fat cells. RSV bilosomes (RB) were prepared as a non-targeted system for comparison. CRB showed nanosize (364.1 nm ±6.5 nm) and high entrapment for both active compounds. Rats treated topically with CRB revealed a significant decrease ( $P = 0.039$ ) in body weight. Histological analysis of the excised skin demonstrated a reduction in the subcutaneous fatty layer thickness and a decrease in the size of connective tissue-embedded fat cells. Kidney histological examination of RB-treated rats showed subcapsular tubular epithelial cells with cytoplasmic vacuolation. This reflects a systemic effect of RSV from the non-targeted RB compared to CRB, which had a targeting effect on the adipose tissue. In conclusion, CAF in CRB significantly enhanced RSV deposition in adipose tissue and assisted its local-acting effect for managing obesity and cellulite.

### 1. Introduction

Obesity is the 5th leading cause of mortality worldwide (Organiza-tion, 2020). It causes physical disabilities such as chronic fatigue, sleep apnea, and poor attention (Field et al., 2001; Knowler et al., 2002, and Calle et al., 2003). Moreover, it may result in the appearance of skin alteration, which is observed widely on the thigh and buttock areas. This mainly appears in women with a phenomenon known as cellulite. Cellulite is depicted as a redistribution of subcutaneous fat in the hypodermis layer resulting from the contraction of connective tissue and fibers due to the expansion of adipose tissue (Hamishshkar et al., 2015).

Herbal drugs are considered a safe approach in managing obesity and cellulite. Caffeine (CAF) is a methylxanthine alkaloid, which is chemically known as 1, 3, 7-trimethylpurine-2, and 6-dione. It is mainly found in coffee, tea, and many drinks. Incorporation of CAF in various topical

cosmetic products was found to prevent excessive fat accumulation in the skin (Carrageta et al., 2018) and manage gynoid lipodystrophy or cellulite (Herman and Herman, 2013). It was reported that CAF causes fat lipolysis and manages cellulite by inhibiting phosphodiesterase enzyme activity. This enzyme is responsible for converting cyclic adenosine monophosphate (cAMP) to Amp; thus, the level of cAMP increases, and adipocyte lipolysis occurs (Herman and Herman, 2013). Moreover, it potentiates fat cell lipolysis by activating lipase enzymes that hydrolyze triglycerides into fatty acids and glycerol (Hexsel, and O. C., Zechmeister do Prado D., 2005; Luebberding et al., 2015). CAF is considered as a non-selective adenosine A1 receptor antagonist (Fredholm and Persson, 1982; Kotańska et al., 2020). These receptors are the most predominant subtype in fat cells (SCHWABE, T. T. A. U., 1980). When CAF binds to adenosine receptors, it antagonizes adenosine action, leading to an increase in the level of cAMP, inhibiting adipogenesis.

**Abbreviations:** CAF, Caffeine; RSV, Resveratrol; RB, Resveratrol bilosomes; CB, Caffeine bilosomes; CRB, Caffeinated-resveratrol bilosomes; cAMP, Adenosine monophosphate; STC, Sodium taurocholate; %EE, Percent entrapment efficiency.

\* Corresponding author.

**E-mail addresses:** [wessam.elrefaie@pua.edu.eg](mailto:wessam.elrefaie@pua.edu.eg) (W.M. El-Refaie), [yosra.elnaggar@pua.edu.eg](mailto:yosra.elnaggar@pua.edu.eg) (Y.S.R. Elnaggar), [habelkader@kku.edu.sa](mailto:habelkader@kku.edu.sa) (H. Abdelkader), [afatease@kku.edu.sa](mailto:afatease@kku.edu.sa) (A. Al Fatease), [ossama.youssef@alexu.edu.eg](mailto:ossama.youssef@alexu.edu.eg) (O.Y. Abdallah).

<https://doi.org/10.1016/j.ijpx.2024.100236>

Received 2 December 2023; Received in revised form 3 March 2024; Accepted 6 March 2024

Available online 13 March 2024

2590-1567/© 2024 The Authors. Published by Elsevier B.V. This is an open access article under the CC BY-NC license (<http://creativecommons.org/licenses/by-nc/4.0/>).

This results in the overexpression of adenosine and leads to the accumulation of intracellular cAMP, by which fat lipolysis occurs (Fredholm and Persson, 1982).

Surveying the literature, two studies concerning nano-technology were conducted on CAF: CAF-loaded niosomes and solid lipid nanoparticles (Hamishehkar et al., 2015; Teaima et al., 2018). These studies aimed to enhance CAF topical permeation deep into skin layers where adipose tissue is located. This resulted in fat loss and management of cellulite appearance. The early report was conducted by Hamishehkar et al., (Hamishehkar et al., 2015), who prepared CAF-loaded solid lipid nanoparticles that showed 94 nm in size and 86% entrapment efficiency. Conventional CAF hydrogel was also prepared for comparison and both preparations were applied to the lumbar regions of obese female rats for 21 days. In contrast to areas treated with CAF-hydrogel, regions treated with CAF-loaded solid lipid nanoparticles showed full lysis of the hypodermis-located adipocyte membrane and a considerable reduction in the bulk of fat tissue.

Another study by Teaima et al. (Teaima et al., 2018) prepared niosomal nano-carrier gels using the thin film hydration technique. Their results showed that after topical application on albino rats for 21 days, the formula succeeded in reducing the thickness of fatty layers compared to the commercial product. However, no studies examined the CAF targeting effect and its ability to enhance nano-carrier deposition in fat cells, improving efficacy.

Resveratrol (RSV) is an antioxidant polyphenol that is mostly found in red grapes. It possesses different anti-obesity mechanisms throughout the adipose cell life cycle (Frankel et al., 1993; Gnad et al., 2014). It has a browning effect through activating PPAR $\gamma$  co-activator 1 $\alpha$  (PGC1 $\alpha$ ), which subsequently enhances uncoupling protein 1 expression and initiates the browning of white adipose tissue (WAT) (Wang et al., 2015). Adipose triglyceride lipase and hormone-sensitive lipase, two necessary enzymes that support fat lipolysis, are directly activated by RSV (Trites and Clugston, 2019).

It is well known that the skin permeation of drugs mainly relies on their physicochemical properties (e.g., lipophilicity, solubility, and molecular weight) (Marjukka Suhonen et al., 1999). Molecular weight drugs higher than 500 Da, those are poorly soluble, and those with high hydrophilicity cannot easily permeate through the skin (Bézivin et al., 2017). Therefore, topical application of both hydrophilic CAF (Log P -0.07) and the poorly soluble RSV is limited. The use of nanotechnology might facilitate their topical delivery.

Phosphatidylcholine and bile salts were reported to have fat lipolysis effects as they act as emulsifying agents that solubilize fats, alter their physicochemical properties, and stimulate their removal through lymphatic drainage (Doris Hexsel et al., 2003; Giovanni Salti et al., 2008). In addition, they can promote drug skin penetration. In our previous research, a novel nanobilosomal formulation was designed to emulate the lipolysis effects of the marketed subcutaneous injections while being non-invasive via topical application (Khalil et al., 2022). The prepared RSV-loaded bilosomes were applied topically to obesity-induced female Wistar rats for a treatment period of 4 weeks. Results showed a detectable decrease in body weight and abdominal circumference. Moreover, histological examination of fat tissue showed a significant reduction in the size of fat cells and browning of white fat cells. RSV-loaded bilosomes more effectively promote lipolysis non-invasively than subcutaneous injections. However, these RSV-loaded bilosomes could not selectively bind to fat cells. Therefore, our aim in this work is to fabricate targeted bilosomal vesicles loaded with RSV and coupled with CAF (CRB) and to compare its cellulite management and anti-obesity effect with caffeine bilosomes (CB) and non-targeted RSV bilosomes (RB). It is the first study to utilize CAF as a targeting agent for fat cells. Additionally, the combination of two active compounds having a fat lipolysis effect loaded on bilosomes might have an improved effect for the non-invasive management of obesity and cellulite.

## 2. Materials and methods

### 2.1. Materials

Caffeine anhydrous was purchased from Titan Biotech Limited, India. *trans*-Resveratrol was bought from Baoji Guokang Bio-Technology Co., Ltd. China. Sodium taurocholate (STC) was supplied by Chem-Impex International, Inc. (USA). Soybean Phosphatidylcholine (Phospholipon® 90 G) was kindly provided from Lipoid GmbH (Ludwigshafen, Germany). Carbopol 940 was obtained from BF Goodrich Company (Saginaw, Michigan, USA).

### 2.2. Animals

The study was conducted using the protocol approved by the Animal Care & Use Committee of the Faculty of Pharmacy, Alexandria University (Approval number: 0620192138). Six groups of 38 mature Wistar female rats, with 155 g average weight at 6 weeks old, were randomly created. Each treated group consists of six rats. Seven rats make up the control groups. The rats were randomly divided into five groups depending on the applied treatment, along with the negative control group of thin rats fed a normal meal (Group 6). In groups 1 and 2, rats were treated with topical application of RSV-bilosomal gel (RB) and CAF-bilosomal gel (CB) respectively. Group 3 represented rats treated with caffeinated-resveratrol bilosomes (CRB), while group 4 represented rats treated with CAF-RSV-gel. The positive control, Group 5, represented the obese non-treated rats fed a HFD. Each group is kept in a cage at a temperature (20 to 25 °C). One day before the treatment, each rat had the abdominal hair removed using a depilatory cream to permit the topical application.

### 2.3. Tailoring and characterization of Caffeinated-resveratrolbilosomal gel (CRB)

#### 2.3.1. Preparation of CRB

Caffeine-integrated resveratrol bilosomes (CRB) were formed using thin film hydration (Shalaby et al., 2020). In this preparation, bilosomes were loaded with two different active compounds: a hydrophilic one (CAF) and a lipophilic one (RSV). Phospholipon 90G (PL 90G) and RSV (with molar ratio 25:1) were dissolved in a 10 mL mixture of chloroform: methanol in a ratio (2:1 v/v) in a 50 mL round-bottom flask. The organic phase was allowed to evaporate under reduced pressure (600 mmHg) in a rotary evaporator at 55 °C until a thin film was obtained on the flask wall. The glass flask was set aside for an hour to guarantee that all traces of organic solvents were eliminated. The resulting film was hydrated using 10 mL phosphate buffer (pH 5.5) containing 10 mg CAF and 62.5 mg STC. Hydration was continued for two hours to allow good mixing of formulation ingredients. The final dispersion was extruded through a Liposome Extruder (ER-1, Eastern Scientific LLC, USA) equipped with a polycarbonate membrane filter (200 nm) at 55 °C (Isailović et al., 2013). After that, the extruded bilosomal dispersions were stored at 4 °C. For comparison, RSV bilosomes (RB) and CAF-bilosomes (CB) were also prepared using the same technique and the same amount of RSV and CAF, respectively.

To prepare bilosomal hydrogel, carbopol 940 polymer was dissolved (1% w/v) in distilled water via 90 min of stirring at 400 rpm using a magnetic stirrer. Then, the pH was adjusted to 6.5 by drop-wise addition of 0.01 M NaOH (Azizi, and E. F., Partoazar A, Ejtemaei Mehr S, Amami A., 2017). Prepared bilosomes were mixed with the prepared Carbopol gel with a ratio (1:1 v/v) by magnetic stirrer so that each 1 ml of the bilosomal gel preparation contains a 1 mg RSV and 0.5 mg CAF. Conventional CAF-RSV gel containing the same drugs concentration was prepared by mixing the prepared carbopol gel (1%w/v) with RSV ethanolic and CAF aqueous solutions.

### 2.3.2. Physicochemical characterization of vesicles

**2.3.2.1. Particle size, polydispersity index, and Zeta potential.** Zetasizer Nano ZS (Malvern, Instruments Ltd., Malvern, UK) was used to determine the zeta potential (ZP), polydispersity index (PDI), and particle size (PS) CRB, RB, and CB (Mohsen et al., 2017). To prevent multi-scattering phenomena, 10 mL deionized water was used to dilute each 1 mL formulation. Three measurements were carried out for each sample, and the findings were given as the mean value  $\pm$  SD.

**2.3.2.2. % Drug Entrapment efficiency (%EE).** Cold centrifugation was conducted at 15,000 rpm for 30 min at 4 °C to separate the prepared vesicles (CRB, RB, and CB) to determine the %EE. Supernatants containing free RSV and/or CAF were carefully withdrawn and suitably diluted with deionized water, and then each drug was separately determined via its own validated HPLC method.

The HPLC system (Agilent) had a reversed-phase column (C18, 5 mm  $\times$  4.6 mm  $\times$  150 mm) and a sensitive diode array detector. For CAF analysis, an isocratic mobile phase (Purified distilled water: methanol; 50:50) was run at a flow rate of 0.9 mL per minute at 40 °C, and the column effluent was analyzed at  $\lambda_{\max}$  272 nm (Davidov-Pardo and McClements, 2014). For RSV analysis, the mobile phase was HPLC grade water with methanol (45:55). The flow rate was 1 mL/min at 30 °C, and the run period was 10 min. The analysis of RSV was performed at  $\lambda_{\max}$  = 310 nm (Algul et al., 2018). The % EE was estimated through:

$$\%EE = \frac{(Total\ drug\ (mg) - free\ drug\ (mg))}{Total\ drug\ (mg)} \times 100.$$

**2.3.2.3. Elucidation of bilosomes' morphology.** A diluted bilosomal sample was applied on a copper grid, then 2% uranyl acetate was used for negative staining. After air dried at room temperature, the samples (CRB, RB, and CB) were observed with transmission electron microscopy (TEM) (Raza et al., 2013; Negi et al., 2017).

**2.3.2.4. Fourier-transform infrared spectroscopy (FTIR).** FTIR spectrum was performed for each of the bilosomes components alone (PL, RSV, CAF, and STC), CAF and STC mixture, dry physical mixture, and the nanobilosomal formulation. This experiment was performed to detect if there is any interaction occurs during the preparation of nanobilosomes. Each sample was placed just below the probe of the FTIR spectrophotometer (Agilent, USA) and scanned over the 4000–500  $\text{cm}^{-1}$  wave-number region.

### 2.4. In vitro release study

The release of both RSV and CAF from the prepared RB, CB, and CRB-gel was determined using the membrane diffusion technique (Mabrouk et al., 2021). A precisely calculated amount of drug-loaded bilosomal gel equivalent to 1 mg RSV and/or 0.5 mg CAF was transferred to a dialysis bag with a 16 mm diameter and 12,000–14,000 Da molecular weight cutoff. Before dialysis, the dialysis bags were soaked in distilled water for 12 h to ensure that the membrane was completely wet. Each drug was analyzed alone using its specified release conditions as follows:

#### 2.4.1. In vitro release for RSV

Dialysis bags were placed in 60 mL of 8:2 v/v mixture of ethanol and PBS (pH 5.5) as a release medium to determine the amount of RSV released from RB and CRB. To guarantee sink conditions, two milliliters were taken out and replaced with a freshly warmed release medium at regular intervals. As mentioned above, withdrawn samples were analyzed for RSV using reverse phase HPLC column (C18, 5 mm, 4.6, 150 mm), at  $\lambda_{\max}$  310. A mixture of methanol and acidified double distilled water as a mobile phase by the ratio (55:45) with a flow rate of 1 mL/min at 30 °C and 10 min run time (Negi et al., 2017).

#### 2.4.2. In vitro release for CAF

To determine the release of CAF from CRB and CB, the dialysis bags were immersed in 12 mL of PBS (pH 5.5), 0.5 mL of the release medium was withdrawn and compensated with an equal volume of fresh medium to ensure sink conditions. As mentioned above, the withdrawn samples were analyzed for CAF using reverse phase HPLC column (C18, 5 mm, 4.6, 150 mm) at  $\lambda_{\max}$  272 nm. The isocratic mobile phase (purified distilled water: methanol; 50:50) was run at flow rate of 0.9 mL per minute at 40 °C and 7 min run time (Hamishehkar et al., 2015).

For both drug releases, the dialysis bags were constantly shaken in a thermostatically controlled shaking water bath at 37 °C  $\pm$  1 °C. All samples were withdrawn at predetermined time intervals. This experiment was performed in triplicate. The results were represented as the mean values of the three runs ( $n = 3$ )  $\pm$  SD.

### 2.5. Ex-vivo permeation study

#### 2.5.1. Human skin preparation

Intact human skin was utilized for studying the permeation and deposition of the ex-vivo drug based on COLIPA guidelines 1997 and OECD guidelines 428–2004 (Benech-Kieffer et al., 1997; OECD Guidelines For The Testing of Chemicals; Skin Absorption: in vitro method, 2011). All individuals who participated in the study gave their informed consent. The obtained skin was separated into whole skin with the subcutaneous fatty tissue and undamaged skin after removing the subcutaneous fats. Ringers' solution was used to clean the skin's surface, then it was washed with saline and left to air dry between two filter papers. After that, it was wrapped in aluminum foil and kept in a polyethylene bag in a deep freezer at  $-20$  °C until it was used (Elnaggar et al., 2011a, 2011b).

#### 2.5.2. Skin permeation and deposition study

Modified Franz diffusion cells were fixed with human skin pieces (either with or without subcutaneous fats) with the stratum corneum side facing the donor compartment. 12 h before the experiment, skin pieces were hydrated using pH 7.4 PBS and left at 4 °C. Afterwards, a fresh pre-warmed medium containing 10 mL of PBS at pH 5.5 for CAF analysis and 8:2 v/v PBS pH 5.5 with ethanol for RSV analysis was used at the receptor compartment. An amount of 350  $\mu\text{L}$  of the prepared bilosomal hydrogel formulations equivalent to 350  $\mu\text{g}$  RSV and 175  $\mu\text{g}$  CAF was applied to the skin surface (1.4  $\text{cm}^2$ ) under non-occlusive conditions. The receptor fluid was maintained at 32  $\pm$  1 °C with a stirring rate at 100 rpm. All the examined formulations were assessed in triplicates. The receptor fluid (200  $\mu\text{L}$ ) was collected at 2, 4, 6, and 8 h, filtered then subjected to HPLC analysis. A fresh-release medium was used to replace the samples that were withdrawn. Results were represented as mean value  $\pm$  SD where  $n = 6$ . The skin permeation of RSV and CAF in CRB-gel formulation was compared with RB-gel and CB-gel formulations, respectively.

The amount of drugs deposited in the skin and fat cells was analyzed according to the same procedures in our previous study (Khalil et al., 2022). Skin samples were detached from Franz diffusion cells, the skin surface was cleaned using a cotton swab immersed with alcohol, and skin and fat tissues were cut as small fragments and mounted in 10 mL alcohol, and the amount of RSV and CAF was determined using HPLC.

After the completion of the ex-vivo investigation, the blue test was performed to confirm the skin integrity throughout the experiment (Raza et al., 2013). A cotton swab soaked in alcohol was used to clean the human skin pieces placed in the diffusion chamber. 250  $\mu\text{L}$  of an aqueous solution of methylene blue (MB, 0.1 g %) was applied onto the skin for half an hour under the same experimental conditions of 32 °C  $\pm$  1 °C and 100 rpm shaking. Following that, MB was removed using PBS and then distilled water. UV–Vis Spectrophotometry at a maximum wavelength of 664 nm was used to determine the amount of MB that had penetrated and permeated the receiver fluid. According to our findings, no dye entered the receiver medium. This demonstrates that the skin

was intact during the experiment time.

## 2.6. In vivo study

### 2.6.1. Fats accumulation and obesity induction

Obesity induction was successfully done according to our previous study (Khalil et al., 2022). This was briefly performed by using a high fat diet (HFD) containing 40% sheep fats mixed with the normal food for 6 weeks. The negative control rats were fed only normal food. For confirmation of obesity induction, an obese and a lean rat were sacrificed, and fat lobes were isolated, weighed, photographed, and examined and compared under an optical microscope.

### 2.6.2. Treatment regimen

Thirty obesity-induced rats were randomly divided into five groups (each was 6 rats) depending on the applied treatment, along with the negative control group of thin rats fed a normal meal (Group 6). In groups 1 and 2, rats were treated with topical application of RSV-bilosomal gel (RB) and CAF-bilosomal gel (CB) respectively. Group 3 represents rats treated with caffeinated-resveratrol bilosomes (CRB), while group 4 represents rats treated with CAF-RSV-gel. The positive control, Group 5, represents the obese non-treated rats fed a HFD.

Throughout the treatment, 2 g of the specified preparations were topically applied once daily to the abdominal region (covering a 3 cm<sup>2</sup> area) for 1 month. Drug-loaded gels contain 1 mg CAF and/or 2 mg RSV. Throughout the course of treatment, HFD meals are continued. Each rat's daily food intake was calculated from the start of the experiment until the end. Each rat received an average of 50 g of HFD for all groups except group 6 (the negative control), which received 50 g of normal forage. The residual forage weight after 24 h was subtracted from the delivered food weight to determine the quantity each rat consumed.

**Daily food consumption in grams** = (Remaining food weight after 24 h – initial delivered food weight)

### 2.6.3. Abdomen circumference and body weight change

All rats had their total body weight and abdomen circumference (AC) measured once a week from the beginning of the experiment till the end. The greatest area of the rat's abdomen was measured for AC with a non-extendable, plastic measuring tape (Novelli et al., 2007; Gerbaix et al., 2010).

The following equations were used to determine the total weight change and % weight change:

Total weight change = (1st treatment day measured weight – Weight measured at each week's end) (Jadeja et al., 2011).

$$\% \text{Weight change} = \frac{\text{Amount of weight change after each week treatment}}{\text{Weight on the 1st treatment day}} \times 100$$

Liu et al. 2000

### 2.6.4. Biochemical analysis

An enzymatic colorimetric test was used to determine the total lipid profile. Once every week, blood samples (2 mL) were collected from the rats' retro-orbital veins. Samples were then centrifuged for 20 min at 4000 rpm (Elnaggar et al., 2011a, 2011b, Teaima et al., 2018). The obtained serum was analyzed for total lipid profile, namely total cholesterol (TC), triglycerides (TG), low-density lipoprotein cholesterol (LDL-C), and high-density lipoprotein cholesterol (HDL-C).

### 2.6.5. Histological study of skin and fat cells

After the treatment, rats were anesthetized using an isoflurane-soaked cotton pad and sacrificed by cervical dislocation. Bilosomal formulations (RB, CB, and CRB) and the gel formulation (CAF-RSV gel) were assessed for their effects on the size, number and color of fat cells via histological evaluation of the excised adipose tissue. As previously noted, the fat lobes separated from the upper half of the limbs were inspected for their weight. Additionally, adipocytes size was estimated through an optical light microscope examination of the isolated adipose tissue. The fat cells' diameter is measured two times. After the calculation of the average diameter of each fat cell, the following equation is used to calculate the average cell diameter:

$$\text{Average diameter of fat cells} = \frac{\text{Total of average diameter for all fat cells}}{\text{Number of fat cells}}$$

Full-thickness skin biopsies were also collected at the end of the treatment. Formaldehyde solution (10% v/v) was used for fixing the specimens. The fixed specimens were embedded in paraffin, cut into 5 μm pieces, and stained with hematoxylin and eosin (H&E). Sections were visualized under the light microscope at 10× magnification. Fields were examined for the integrity of the skin and the thickness of adipose tissue. Connective tissue that is present at the border between the dermis and the adipose tissue and is known as fibrous septae was also examined. It gives an insight into the development of cellulite (Omi et al., 2013).

## 2.7. Detection of organ toxicity

The livers and kidneys of the sacrificed rats were isolated and visually inspected for any abnormalities in their size, color, and surface structure. Additionally, isolated organs were histologically examined under an optical microscope. First, they were fixed in formaldehyde (10%), immersed in paraffin, then cut and stained with H&E (El-Mezayen et al., 2018). A light microscope was used to examine the prepared sections (Olympus Germany).

## 2.8. Stability study

The prepared formulations were kept in glass screw-capped containers at 4 °C for 6 months. The physical stability in terms of particle size, zeta potential, PDI, and %EE was examined at predefined time intervals. Additionally, the formulations underwent periodic visual checks for aggregation or any changes in the formulations.

## 2.9. Statistical analysis

In order to analyze the data, Microsoft Excel 2017 was used. The mean and standard deviation were used to express the results. A two-tailed, unpaired student *t*-test was used to evaluate statistically significant differences with *P* < 0.05 expressed as the significance level.

## 3. Results and discussion

### 3.1. Preparation and characterization of caffeinated-resveratrol bilosomes

Novel caffeinated-resveratrol bilosomes (CRB), resveratrol bilosomes (RB), and caffeine bilosomes (CB) were prepared by thin film hydration technique using STC as a bile salt. The bilosomal formulations

were further mixed with Carbopol 940 polymer with a concentration of 1 g % with a volume ratio (1:1 v/v) with final viscosity equal to 0.38 P to be suitable for topical application. This was in accordance to Kim et al. who stated that; the value between 0.38 and 0.39 P was reported to be an ideal viscosity value for topical gel formulation developed using carbopol polymers (Kim and Park, 2003).

The idea of combining both drugs in the same formulation without affecting each other's entrapment came from their different physico-chemical properties. RSV is a lipophilic drug; its solubility was determined as  $0.15 \pm 0.2$  mg/mL in PBS pH 5.5. So, it is assumed to be entrapped in the phospholipid bilayer of RB formulation. In contrast, for CB nanovesicles, CAF is a relatively polar compound with pKa 10.4 (Latosinska et al., 2014); that is partially ionized at pH 5.5 and carries a positive charge due to the presence of a nitrogen atom in the xanthine group. Therefore, CAF can be entrapped in the inner core of nanobilosomes with a small amount adsorbed on the outer surface and around the phospholipid bilayer.

In the case of CRB, where both RSV and CAF are present, due to the high negativity of bilosomes surface by the presence of phosphate group of phospholipid, bile salts, and RSV; a high amount of positively charged CAF tends to be adsorbed on the vesicle surface and forms a layer which coats the prepared bilosomes. Size, ZP, and TEM images will further confirm this.

### 3.1.1. Particle size, PDI, and ZP

CRB particle size was determined using the dynamic light scattering technique. The prepared formulation had PS equal to ( $364.1 \text{ nm} \pm 6.5 \text{ nm}$ ), with PDI  $0.3 \pm 0.1$ . This size is higher than RB ( $269 \text{ nm} \pm 3.2 \text{ nm}$ ) and CB ( $253.1 \text{ nm} \pm 9.8 \text{ nm}$ ). This might indicate the entrapment of

RSV, and CAF integration inside and around the vesicles, as TEM will further confirm.

Concerning ZP value, by comparing the ZP of the prepared RSV bilosomes (RB,  $-49.9 \text{ mV} \pm 3.7 \text{ mV}$ ) to CRB ( $-28.1 \text{ mV} \pm 2.7 \text{ mV}$ ) and CAF bilosomes (CB,  $-11.9 \text{ mV} \pm 3.5 \text{ mV}$ ), a significant decrease ( $P = 0.023$ ) in the negative ZP value was observed. RB has a higher negative ZP due to the lipids' phosphate group (phospholipon 90 G, PL 90G) (Liu et al., 2000), bile salt (STC) (Aburahma, 2016; Mohsen et al., 2017), and RSV hydroxyl groups. For CRB and CB, a decrease in the negativity was observed due to the presence of CAF adsorbed on the outer surface of bilosomes. This further confirms CAF coating to the nanovesicles.

### 3.1.2. Entrapment efficiency (%EE) of both RSV and CAF

The % entrapment of CAF and RSV in the prepared CRB formulation was found to be ( $68.7 \pm 4.7\%$ ) and ( $94.1 \pm 8.5\%$ ) respectively. This high entrapment in bilosomal system might be due to the lipid bilayer that could solubilize and accommodate RSV as a lipophilic drug inside it. Hydrophilic drugs such as CAF can either be entrapped in the inner aqueous core or adsorbed on the surface of the vesicles. Moreover, adding bile salts is thought to solubilize and accommodate both lipophilic and hydrophilic drugs as they act as surface active agents (Ahad et al., 2018). They might increase the % EE by the interaction of the drug with either the surfactant's hydrophilic head group or its lipophilic tail according to the drug's nature (Teaima et al., 2018).

It is worth noting that the combination of both RSV and CAF in the same formulation did not alter the entrapment of each alone. For CAF-bilosomes (CB), the % EE of CAF was  $72 \pm 3.1\%$ . On the other hand, the % EE of RSV in RSV-bilosomes (RB) was  $95.3 \pm 2.1\%$ .

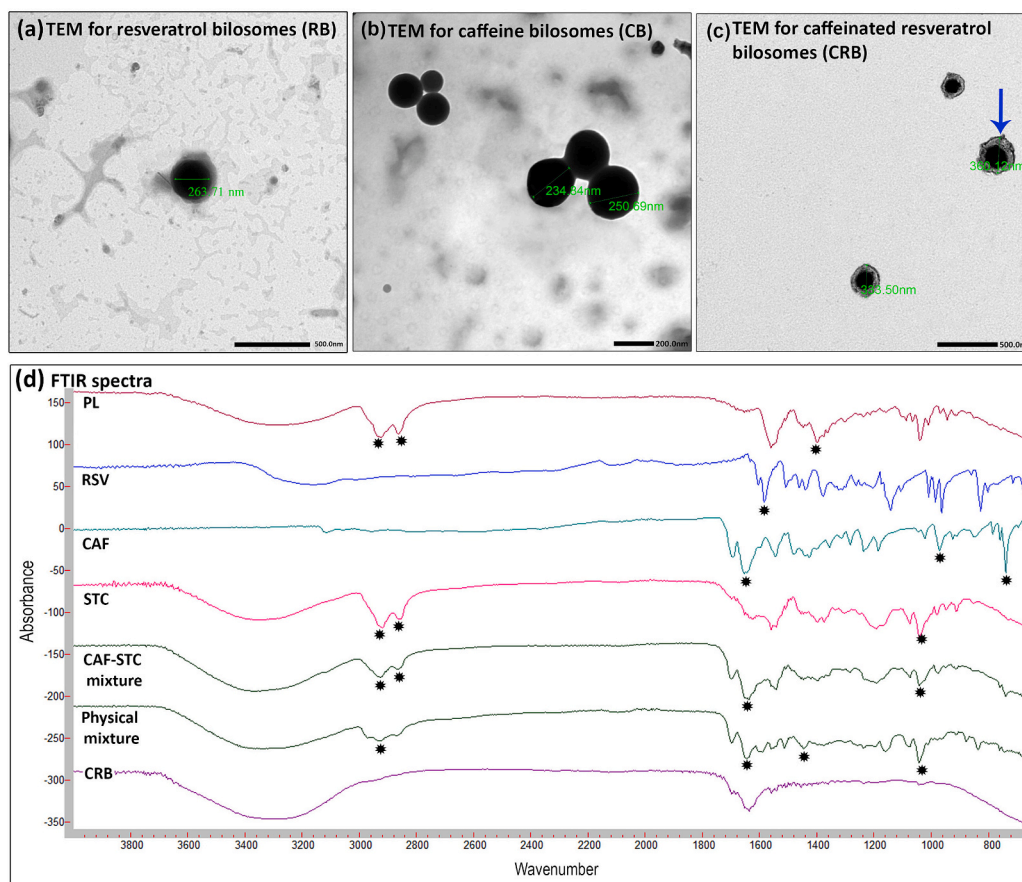


**Fig. 1.** Transmission electron micrograph of (a) RSV bilosomes (RB), (b) CAF bilosomes (CB), and (c) caffeinated-resveratrolbilosomes, the blue arrow refers to the adsorbed caffeine layer on the outer surface of the vesicle. (d) Fourier-transform infrared (FTIR) spectrum for PL, RSV, CAF, STC, CAF-STC, physical mixture, and CRB formulation. (For interpretation of the references to color in this figure legend, the reader is referred to the web version of this article.)

### 3.1.3. Morphological characterization

Morphological examination confirmed the formation of uniform round vesicles. The photomicrographs (Fig. 1) demonstrated a spherical vesicle structure and a homogeneous size distribution. By comparing the micrograph of CRB (Fig. 1c) with that of RSV bilosomes (RB) (Fig. 1a) and CAF-bilosomes (CB) (Fig. 1b), a thick cloudy layer appeared that coats the vesicles' surface. This confirms the formation of a CAF coat around the vesicles. RSV, the negatively charged lipophilic drug, might push CAF out to the surface. As a result, a large amount of CAF was adsorbed on the outer layer of bilosomes, and ionic interactions are likely to occur between CAF (positively charged) and the negatively charged bilosomes. This resulted in the formation of an adsorbed layer of CAF surrounding the surface of nanovesicles.

### 3.1.4. Fourier-transform infrared spectroscopy (FTIR)

FTIR analysis was employed to study potential interactions among the prepared bilosomes' additives (PL, RSV, CAF, and STC). Physical mixture of CAF and STC, physical mixture of all ingredients, and caffeinated-resveratrol bilosomal formulation (CRB) were also performed, as shown in (Fig. 1d).

Phosphatidylcholine (PL) spectrum was recorded, and it showed strong sharp peaks at  $2920\text{ cm}^{-1}$ ,  $2851\text{ cm}^{-1}$ , and a weak peak at  $1378\text{ cm}^{-1}$  due to the stretching and deformation of the methyl group (Elnaggar et al., 2011a, 2011b; Komeil et al., 2021). P=O stretching appeared at ( $1299\text{--}1250\text{ cm}^{-1}$ ) in addition to a strong broad band for quaternary ammonium.

RSV spectrum showed three characteristic intense bands at  $1605$ ,  $1589$ , and  $1384\text{ cm}^{-1}$  corresponding to C=C aromatic double bond stretching, C=C, and C=O stretching (Vittorio Bertacche et al., 2006).

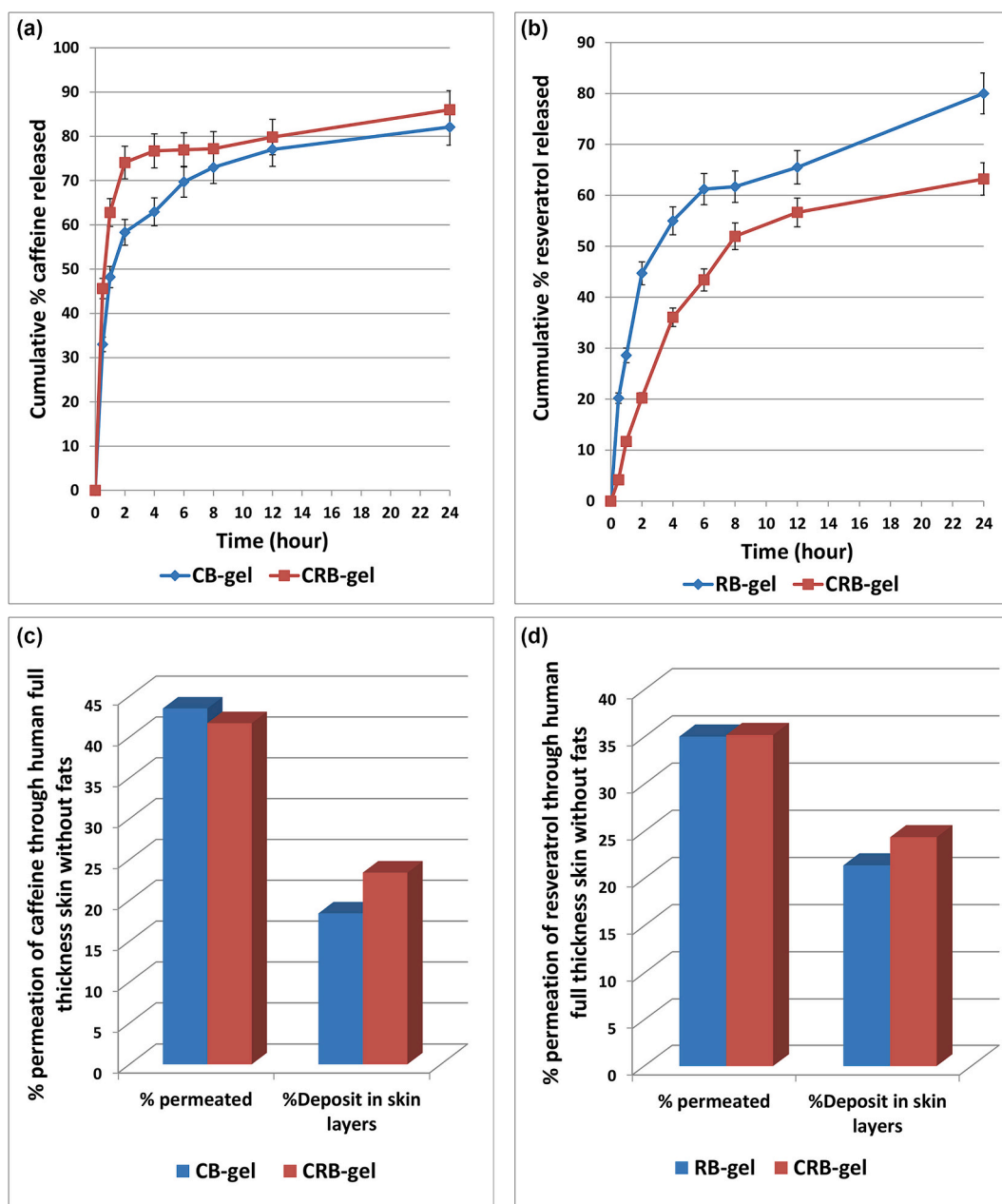


Fig. 2. In vitro release of (a) CB-gel and CRB-gel using dialysis bag technique in phosphate buffer (PH 5.5), (b) RB3-gel and CRB-gel using dialysis bag technique in PBS PH (5.5) and ethanol as a release medium with volume ratio (8:2 v/v) at  $37^{\circ} \pm 1\text{C}$  for 24 h, (c) Average % of caffeine permeated and deposited in skin without fats from CB-gel and CRB-gel and (d) Average % of resveratrol permeated and deposited in skin without fats from RB-gel and CRB-gel after ex vivo permeation study at  $32^{\circ} \text{C} \pm 1^{\circ} \text{C}$ . Results represent means  $\pm$  standard deviations (SD),  $n = 3$ .

CAF spectrum showed strong vibrational bands at  $970\text{ cm}^{-1}$  and  $925\text{ cm}^{-1}$  that are assigned to the N=C-H and N-C-H deformation vibrations. These vibrations occur in the imidazole ring. Strong bands were observed at  $1650\text{ cm}^{-1}$  and at  $1545\text{ cm}^{-1}$ , which are considered to be due to C=O asymmetric and symmetric stretching vibrations. The frequency observed at  $740\text{ cm}^{-1}$  is assigned to be due to O=C-C bending of the pyrimidine ring (Gunasekaran et al., 2005).

Sodium taurocholate (STC) spectrum showed three distinctive features at  $2936$ ,  $2863$ , and  $1562\text{ cm}^{-1}$ , which correspond to the CH stretching vibration and the COO- stretching vibration modes (Yang et al., 2005). Moreover, a characteristic peak at  $1186\text{ cm}^{-1}$  corresponding to SO<sub>3</sub>-stretching was also observed (Muzzarelli et al., 2006).

The characteristic peaks for the binary mixing of CAF and STC remain unchanged. This suggests that there was no interaction between them.

For caffeinated-resveratrol bilosomal formulations (CRB), the characteristic peaks of IR-spectrum disappeared when compared to the physical mixture. This indicates a sort of interaction and/or complexation that takes place through the preparation of bilosomes.

### 3.2. In-vitro release study

CRB-gel formulation has a significant ( $P = 0.041$ ) increase in CAF release rate compared to CB-gel (Fig. 2a). This high % drug release in CRB-gel formulation might be due to the presence of a considerably high amount of CAF surrounding the surface of bilosomes. CAF has a good solubility in the phosphate buffer; thus, it diffuses through the dialysis bag to the release medium, where the drug dissolves.

On the other hand, a significant ( $P < 0.05$ ) decrease in %RSV release compared with RB-gel was observed (Fig. 2b). This low % of drug released may be attributed to the presence of a CAF coat on the bilosomes surface, which hinders and delays RSV diffusion to the release medium.

### 3.3. Skin penetration and deposition study

#### 3.3.1. Full-thickness human skin without fats

The % drug penetrated and localized in the fat-trimmed human skin for CAF and RSV from CRB-gel formulation were compared with CB-gel and RB-gel, respectively (Fig. 2c and d). Results demonstrated an insignificant ( $P > 0.05$ ) difference in the total % drug permeated to receiver fluid and the total % drug deposited in the skin. This indicates, in the absence of fat tissue, that the targeting effect of CAF in CRB is not obvious, as no adenosine receptors are found.

#### 3.3.2. Drug permeation and deposition in a full thickness of human skin

The presences of both CAF and RSV together in CRB-gel formulation significantly change drug distribution in skin attached to fats compared with using CAF only in CB-gel or RSV only in RB-gel (Fig. 3a and c).

For CAF, a significant ( $P = 0.011$ ) decrease in % CAF permeated to receiver fluid for CRB-gel compared to CB-gel. Moreover, no drug was permeated to the receiver medium during the first 4 h of the experiment (Fig. 3b). This delay might be due to the fact that fats make a barrier that delays the passage of nanovesicles to the receiver medium. Moreover, CAF has a great affinity to adenosine A1 receptors that are found in adipose tissue. As a result, nanovesicles needed a longer time to reach

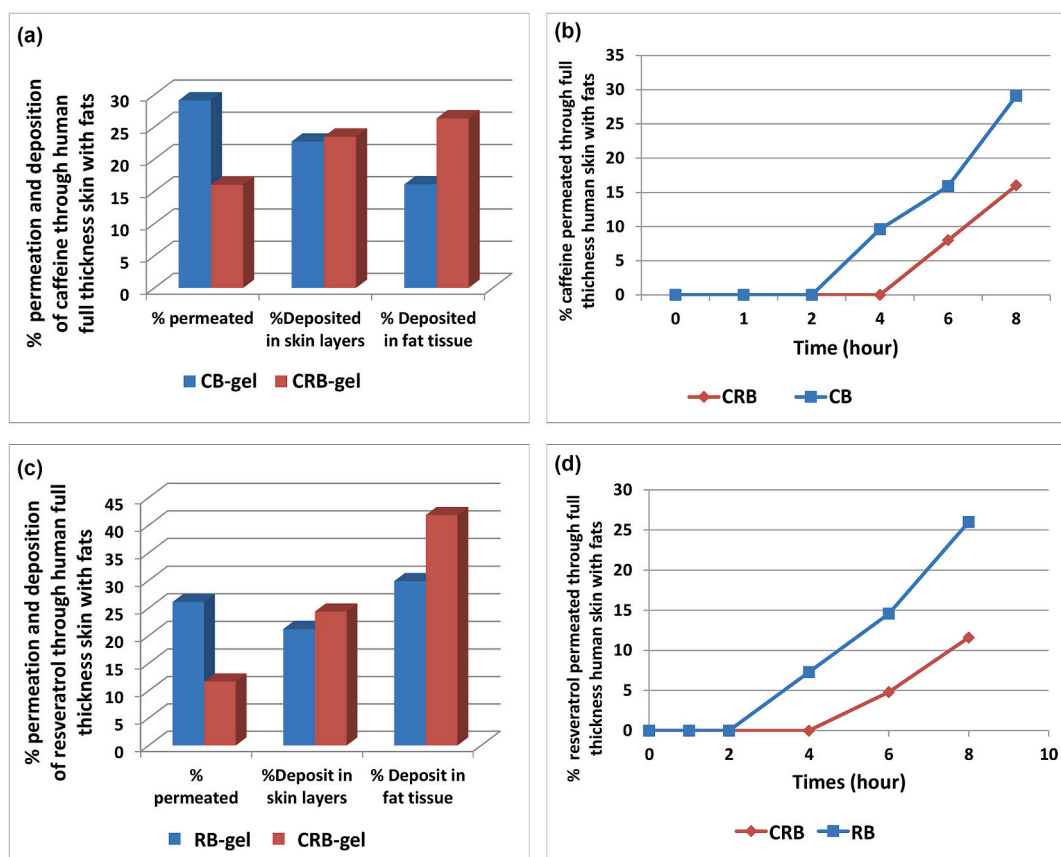


Fig. 3. (a) Ex vivo skin permeation of caffeine from CB-gel and CRB-gel in PBS (pH 5.5) release medium, (b) Average % of caffeine permeated to receptor fluid and deposited in skin and fat tissue from CB-gel and CRB-gel, (c) Ex-vitro skin permeation of resveratrol from RB-gel and CRB-gel in release medium contains mixture from PBS (PH 5.5) and ethanol with ratio 8:2 (v/v). (d) Average % of resveratrol permeated to receptor fluid and deposited in the skin and fat tissue from RB-gel and CRB-gel. Ex-vitro permeation study was performed through full thickness human skin with fats using Franz diffusion cell at  $32\text{ }^{\circ}\text{C} \pm 1\text{ }^{\circ}\text{C}$ , the represented amounts of drugs permeated and deposited were after 8 h study. Results represents means  $\pm$  standard deviations (SD),  $n = 3$ .

the receiver medium.

A significant ( $P < 0.05$ ) increase in % CAF deposited in fats for CRB-gel compared to CB-gel was observed. While the % CAF deposited in the skin was insignificantly ( $P > 0.05$ ) changed (Fig. 3a). This enhancement in % CAF deposited in fats might be due to the high affinity of CAF to bind with adenosine receptors. Moreover, RSV increased the lipophilicity of nanovesicles, which dragged the nanosystem deep into fats and deposited there other than permeating to the receiver fluid.

On the other hand, integration of CAF in CRB-gel formulation affects the % RSV permeated to receiver medium and % deposit in skin and fats compared with RB-gel formulation (Fig. 3c). A noticeable delay in the drug release pattern was observed; no drug was permeated to the receiver medium during the first 4 h of the experiment. Moreover, a significant ( $P = 0.047$ ) decrease in RSV permeated in CRB-gel was observed compared to RB-gel (Fig. 3d). In contrast, % RSV deposited in skin and fats significantly increased in CRB-gel compared to RB-gel (Fig. 3c). This increase in % RSV deposited in skin and fats might be attributed to the incorporation of CAF in nanovesicles. CAF acts as a non-selective adenosine A1 receptor antagonist; once CRB penetrates the skin, CAF coating the outer surface of bilosomes drags the nanovesicles and directly targets fat cells, where CAF binds to adenosine receptor and RSV deposits in fats.

Although the % of drug penetrated and localized in the skin significantly differs in CRB-gel compared to CB-gel and RB-gel. However, the total amount of drugs distributed was nearly the same. The total amount of CAF penetrated and localized in both skin and fats was  $67.9\% \pm 3.8$  in CRB-gel and  $65.7\% \pm 9.5$  in CB-gel, while the total amount of RSV permeated and deposited was  $76.9\% \pm 3.2$  and  $77.2\% \pm 5.7$  corresponding to CRB-gel and RB-gel respectively. This proves that CAF has a high targeting affinity to fats, resulting in a localization effect instead of permeation to receiver fluid.

### 3.4. Stability test

CRB formulation was evaluated for its stability for 6 months. A non-significant change in the particle size, ZP, and % entrapment efficiency (%EE) were recorded over 6 months (Table 1). Insignificant change in % EE is attributed to the presence of CAF in the charged form adsorbed on the bilosomal surface forming a protective coat, resulting in the decrease in drug leakage from the inner core (CAF) or phospholipid bilayer (RSV). Additionally, as negatively charged nanoparticles are more resistant to accumulation than uncharged ones, vesicles' stability may be linked to their strong negative charge. Furthermore, bile salts may help to increase the stability via their integration within the phospholipid bilayer, causing a steric stabilization that decreases vesicles' fusion.

### 3.5. In vivo study

#### 3.5.1. Obesity induction evaluation

Throughout the 6-week fat-induction period, rats fed a HFD showed a significant ( $P < 0.05$ ) increase in the total body weight compared to the negative control group that was fed on the standard forage (Supplementary Fig. 1S). This could be attributed to the high fat content introduced in their food. Extra fats are higher than their bodies need and tend to accumulate as fat droplets in adipose tissue (Carreiro and

**Table 1**

Particle size, % entrapped efficiency, and zeta potential determined for caffeinated resveratrol bilosomes formulation for 0, 3, and 6 months at 4 °C. Data represent means  $\pm$  SD,  $n = 3$ .

Time	Particle size (nm)	% Entrapment efficiency (%EE)		Zeta potential (mV)
		RSV	CAF	
0 months	364.1 $\pm$ 6.5	94.1 $\pm$ 8.5	68.7 $\pm$ 4.7	-28.1 $\pm$ 2.7
3 months	376 $\pm$ 10.6	94.1 $\pm$ 11.5	67.3 $\pm$ 13.2	-28.1 $\pm$ 3.7
6 months	381.2 $\pm$ 9.1	94 $\pm$ 13.9	64.9 $\pm$ 5.9	-27.9 $\pm$ 8.1

Buhman, 2019, Khalilet al. 2022). Moreover, the isolated subcutaneous fat lobes showed a large size and a significant ( $P = 0.036$ ) higher weight in obese rats compared to the small size in lean rats.

Daily food intake demonstrated a non-significant change ( $P = 0.009$ ) among the treated groups (groups 1 to 4) and group 5 (the positive control).

The HFD was  $43.9 \pm 1.5$  g/day for the treated rats and  $44.4 \pm 2.3$  g/day for the positive control group, respectively. The daily food consumption for the negative control group (group 6) was  $(22.8 \pm 1.9$  g/day). These findings suggest that the amount of food consumed each day is unaffected by loaded drugs.

Rats' physical appearance and behavior were normal within the treatment period. Obese rats were big and showed some laziness due to their obvious weight gain.

#### 3.5.2. Weight change

% weight change for all rats was calculated weekly. Rats showed different weight change profiles throughout the treatment period. After treatment, groups 1, 2, and 3, treated with drug-loaded bilosomal formulations, demonstrated a significant ( $P = 0.022$ ) body weight loss compared to group 4, treated with conventional gel and to group 5 of obese rats, as revealed in Table 2.

A significant ( $P < 0.05$ ) decrease in rats' body weight was observed during 4 weeks of treatment for groups 1, 2, and 3, as shown in Table 2. The body weight decrease in group 1 (rats treated with RB gel formulation) might be due to RSV loading in bilosomes. RSV-loaded bilosomes can deeply penetrate the skin to adipose tissue, where fat lipolysis occurs. In group 2, rats treated with CAF bilosomes-gel formulation (CB), their reduced body weight reflected the affinity of bilosomes in entrapping CAF effectively and enhancing its permeation through the skin.

For group 3, rats treated with caffeinated-resveratrol bilosomes (CRB) showed the highest weight loss effect. This might be due to the combined effect of CAF and RSV in fat lipolysis. According to our ex-vivo permeation study, a high amount of CAF and RSV were deposited in the adipose tissue. The presence of adenosine receptors enhances drug deposition in fat cells.

In contrast, in rats treated with a conventional CAF-RSV-gel (group 4) and untreated obese rats (group 5), a significant ( $P = 0.038$ ) increase in their body weight was observed. The increase in body weight for group 4 reflects poor drug penetration from conventional topical gel formulations. In the case of an untreated obese group, their total body weight increased due to the continuous intake of HFD with no treatment.

#### 3.5.3. Abdominal circumference

A helpful tool for predicting fat mass could be the abdominal

**Table 2**

The average % weight change throughout the treatment period (4 weeks). Data represent means  $\pm$  SD,  $n = 3$ .

Group number	Applied treatment	Weight before treatment (g)	Weight after treatment (g)	% weight change
Group 1	Resveratrol bilosomal gel (RB gel)	276.2 $\pm$ 4.4	221.8 $\pm$ 2.2	-19.7
Group 2	Caffeine bilosomal gel (CB gel)	266.3 $\pm$ 3.5	241.3 $\pm$ 1.5	-9.4
Group 3	Caffeinated-resveratrol bilosomal gel (CRB gel)	284 $\pm$ 4.4	197.5 $\pm$ 2.9	-30.5
Group 4	Caffeine resveratrol conventional gel (CAF-RSV gel)	271.9 $\pm$ 2.8	341.6 $\pm$ 3.1	+20.4
Group 5	-	241.6 $\pm$ 3.6	340.3 $\pm$ 3.5	+29
Group 6	-	168.7 $\pm$ 4.03	193.8 $\pm$ 4.4	+14.9

\* (+) means an increase in body weight.

\* (-) means a decrease in body weight.

circumference (AC). (Gerbaix et al., 2010) Before treatment, the average initial AC for all the obesity-induced rats was  $22.13 \pm 2.1$  cm. The different treatment potentials of the applied formulations can be discussed by the varied AC results that were obtained.

Groups 1 and 2 treated rats with RB-gel and CB-gel, respectively, showed a slight significant decrease ( $P < 0.05$ ) in AC. After applying treatment for 4 weeks, their average abdominal circumferences were  $20.9 \pm 0.9$  cm and  $21 \pm 2.5$  cm, respectively.

In group 3, CRB hydrogel-treated rats exhibited the highest decrease in AC value compared to other groups. Their AC value significantly decreased from  $24.4 \pm 2.2$  cm to  $16.7 \pm 1.4$  cm. Moreover, an insignificant difference between the AC value of group 3 after treatment ( $16.7 \pm 1.4$  cm) and the negative control group ( $15.9 \pm 3.8$  cm) was observed. As previously discussed, this is due to the combined effect of both CAF and RSV in fat lipolysis. In addition, CAF has a targeting affinity to adenosine receptors on fat cells, enhancing drug deposition there.

### 3.5.4. Biochemical analysis

The normal serum lipid profiles for Wistar rats are 70–120 mg/dl for TG, 50–250 mg/dl for TC, HDL is up to 30 mg/dl (Siques et al., 2014), and LDL is 25–100 mg/dl (Ihedioha et al., 2013). The rats treated with the prepared formulations showed different serum profiles (Table 3). Rats treated with the traditional CAF-RSV-gel preparation (groups 4) and obesity-induced rats (group 5) both revealed significant ( $P = 0.041$ ) increases in their TC, TG, and low LDL levels as well as significant ( $P < 0.05$ ) decreases in HDL levels.

The serum lipid profile of the rats treated with the drug-loaded bilosomes hydrogel formulations (groups 1, 2, and 3) did not significantly differ ( $P > 0.05$ ) before and after treatment. Despite receiving HFD throughout the treatment, rats treated with drug-loaded bilosomes had an insignificantly changed serum lipid profile. This might be because loaded bilosomal formulations have a high local lipolysis effect. As adenosine A1 and A2A receptors are present, loaded drugs (RSV and CAF) have a high affinity to deposit in adipose tissue.

### 3.5.5. Isolated fat lobes average weight and histology

The treated groups showed differences in the average weight, number, and diameter of the isolated fats (Fig. 4a). Obese rats' fat cells (group 5) were found to be few ( $26 \pm 2$ ), large in size ( $127.45 \pm 8.36$   $\mu\text{m}$ ) with average weight ( $25.94 \pm 3.38$  g) compared to normal rats (group 6), which were smaller in size ( $81 \pm 11.96$   $\mu\text{m}$ ) with a high number ( $40 \pm 6$ ) and lower average weight ( $16.82 \pm 0.54$  g).

Rats administered conventional drug-loaded gel preparation (group 4) did not significantly ( $P = 0.041$ ) vary from the positive control group in terms of average size ( $123 \pm 9.77$   $\mu\text{m}$ ), average weight ( $23.79 \pm 1.57$  g) or average number of cells ( $25 \pm 3$ ). On the other hand, groups treated with bilosomal gels either loaded with RSV alone (group 1), CAF alone (group 2), and combined CAF and RSV (group 3) demonstrated a significant fat cells diameter reduction and an increase in their number when compared to obesity-induced rats (group 5) and the group treated

with drug-gel preparation (group 4).

Rats treated with CRB-gel (group 3) showed the least average diameter ( $103.38 \pm 6.92$   $\mu\text{m}$ ) and the highest number of fat cells ( $37 \pm 8$ ) compared to group 1 and group 2, as shown in Fig. 4a. This is due to the dual fat lipolysis effect of both RSV and CAF in the same bilosomal formulations.

Moreover, the browning effect was significantly observed in group 3 (Fig. 4c) compared to the obese non-treated rats in group 5 (Fig. 4b). As previously reported, the browning effect is due to the presence of RSV in the CRB bilosomal formulation, which acts by the activation of mitochondrial biogenesis which converts white adipose tissue (WAT) into brown adipose tissue (BAT). In addition, RSV is a selective agonist of the adenosine A2A receptor. RSV can increase the levels of adenosine in adipocytes, causing their browning. This result confirms our previous study that studied the effect of RSV- bilosomal gel on the lipolysis and browning of obesity-induced fat cells (Khalil et al., 2022).

Also, it should be noted that Fig. 4c showed the presence of CRB bilosomes deposited in the adipocytes. This reflects the high affinity of (CRB) to deposit in fat cells other than loaded bilosomal formulations RB and CB. This confirms the targeting effect of CAF on adenosine A<sub>1</sub> receptors found in fat cells. CAF is considered a non-selective adenosine A1 receptor antagonist (Fredholm and Persson, 1982; Kotańska et al., 2020). Adenosine A1 receptors are the most predominant subtype in fat cells (Schwabe 1980). When CAF binds to adenosine receptors, it antagonizes adenosine action, leading to an increase in the level of cAMP; inhibiting adipogenesis. This results in the overexpression of adenosine and leads to the accumulation of intracellular cAMP, by which fat lipolysis occurs (Fredholm and Persson, 1982).

### 3.5.6. Histological examination of skin biopsies

All of the rats' full-thickness skin samples examined histologically showed intact epidermis and no inflammation. Rats that were treated with conventional gel formulations, obese rats, drug-loaded bilosomes, and normal rats all showed significant differences (Fig. 5). Normal rats (Fig. 5a) had normal skin and a thin layer of subcutaneous fat. Fat cells were not embedded in the connective tissue. Obese rats displayed a thick subcutaneous fat layer, vertical stretching of the superficial fat lobules pouching connective tissue outwards, and the presence of characteristic adipocytes in the connective tissue that indicates the incidence of cellulite (Fig. 5b) (Quatresouz et al. Vittorio Bertacche et al., 2006). In comparison to untreated rats, rats given conventional gel preparations displayed a thickening epidermis and a noticeably thick subcutaneous fat (Fig. 5c). This illustrates how ineffective conventional gel formulations are in penetrating the skin's layers and accumulating in the adipose tissue where fat lipolysis takes place.

In contrast to obese rats, CRB-treated rats (Fig. 5d) showed a thin layer of subcutaneous fat, and the accumulation of nanobilosomes in adipose tissue was also noted. This confirms that CRB has a drug-targeting effect on adipose tissue where the fat lipolysis effect occurs. The connective tissue showed the presence of fat cells embedded in it, which are smaller in size compared to the obese rats. This could indicate

**Table 3**

Monitoring of total cholesterol (TC), triglycerides (TG), low-density lipoprotein (LDL-C), and high-density lipoprotein (HDL-C) before and after 4 weeks of treatment. Data represent means  $\pm$  SD,  $n = 3$ .

Group No.	TC (mg/dl)		TG (mg/dl)		LDL-C (mg/dl)		HDL-C (mg/dl)	
	Pre-treatment	Four weeks post-treatment	Pre-treatment	Four weeks post-treatment	Pre-treatment	Four weeks post-treatment	Pre-treatment	Four weeks post-treatment
1	143 $\pm$ 10.1	121 $\pm$ 11.8	75 $\pm$ 6.5	86 $\pm$ 13.2	99 $\pm$ 3.4	107 $\pm$ 1.1	39 $\pm$ 2.8	39 $\pm$ 3.5
2	129 $\pm$ 12	132 $\pm$ 23.2	98 $\pm$ 15	106 $\pm$ 14.9	114 $\pm$ 2.9	109 $\pm$ 10.6	32 $\pm$ 5.9	34 $\pm$ 1.9
3	157 $\pm$ 16.7	159 $\pm$ 9.2	86 $\pm$ 7	97 $\pm$ 14.3	81 $\pm$ 4	85 $\pm$ 9.5	43 $\pm$ 1.9	42 $\pm$ 8.9
4	165 $\pm$ 12.7	219 $\pm$ 11.8	88 $\pm$ 13	122 $\pm$ 9.8	115 $\pm$ 13.9	142 $\pm$ 17.4	42 $\pm$ 8.2	29 $\pm$ 0.8
5	191 $\pm$ 13.8	251 $\pm$ 3.5 <sup>a</sup>	98 $\pm$ 10.3	137 $\pm$ 7.4 <sup>a</sup>	103 $\pm$ 7.8	155 $\pm$ 0.6 <sup>a</sup>	44 $\pm$ 1.2	20 $\pm$ 1.8 <sup>a</sup>
6	55 $\pm$ 8.8	68 $\pm$ 3.3 <sup>a</sup>	53 $\pm$ 3.5	61.2 $\pm$ 8 <sup>a</sup>	40 $\pm$ 3.5	47 $\pm$ 10.1 <sup>a</sup>	44 $\pm$ 3.6	42 $\pm$ 8.7 <sup>a</sup>

<sup>a</sup> No treatment was applied.

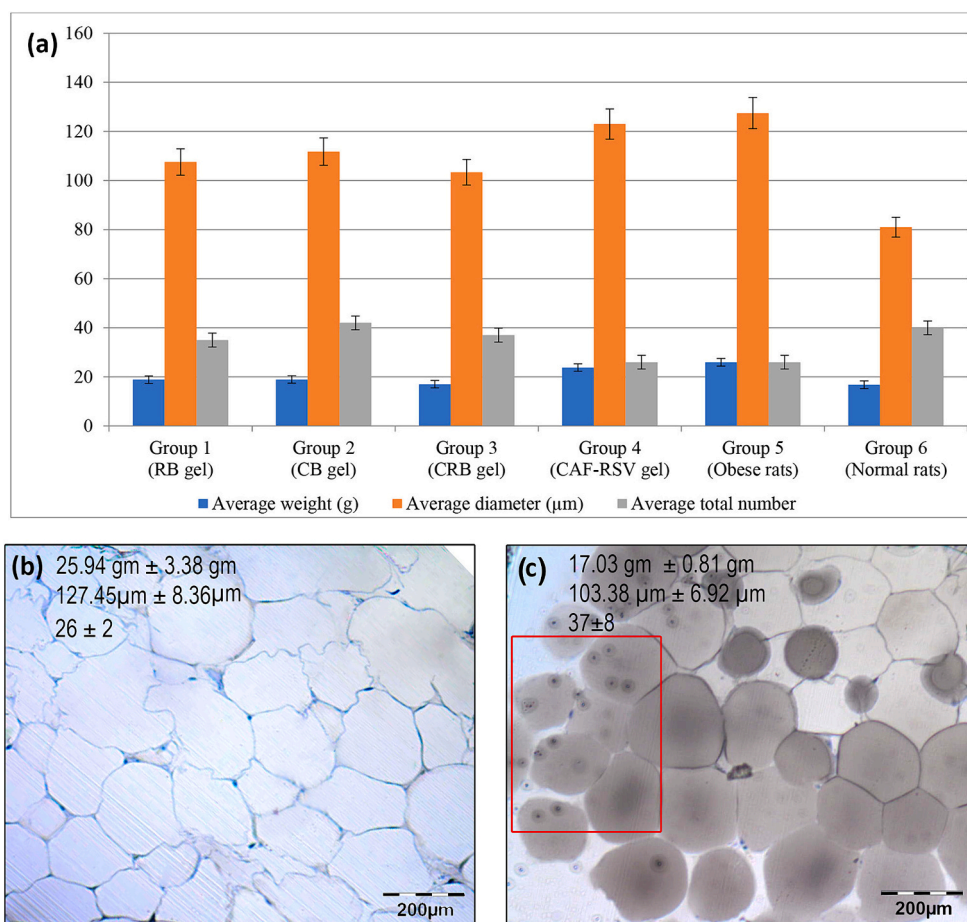


**Fig. 4.** (a) A bar chart showing the average weight (g) of isolated fat lobes, average diameter ( $\mu\text{m}$ ) and the average total number of fat cells in an area of  $25 \mu\text{m}$  for all study groups. Results represent means  $\pm$  standard deviations (SD),  $n = 3$ . (b) and (c) Histological examination of isolated adipose tissue stained with Prussian blue at x10 magnification for obese rats (b), and rats treated with CRB gel (c); the marked section in red shows deposited vesicles in the fat cells. Numbers on the top of figures (b) and (c) indicate the average weight (g) of isolated fat lobes, average diameter ( $\mu\text{m}$ ), and the average total number of fat cells, respectively in the specified area. (For interpretation of the references to color in this figure legend, the reader is referred to the web version of this article.)

the ability of the prepared drug-loaded bilosomes (CRB) to manage cellulite.

### 3.6. Detection of organ toxicity

In the liver, upon their visual inspection, no difference was observed in the color and the external anatomy between all groups. Moreover, normal liver parenchyma with hepatocytes arranged in cords around the central vein and intact portal tract was observed in the histological examination of rats treated with drug-loaded bilosomes and rats treated with drug-gel preparations compared to normal rats (Fig. 5e and f).

For kidneys, the visual inspection did not show any abnormalities in their shape. Histological examination of obese rats, normal rats, and rats treated with CAF-RSV-gel, CB gel, and CRB gel showed normal renal tissue with intact viable glomeruli tubules (Fig. 5g). For rats treated with RSV bilosomal gel (RB gel), the subcapsular tubular epithelial cells showed a mild cytoplasmic vacuolation (Fig. 5h). This might reflect a slight systemic effect of RSV in RB gel. RB might have less targeting effect on adipose tissue compared to CB gel and CRB gel; a small amount of RB could pass to the systemic circulation, reach the kidney, and tubular vacuolation occurred (Crowell et al., 2004). This proves that CAF in CRB plays an important role in the targeting and deposition of RSV in adipose tissue and assists its local acting effect in the management of obesity; avoiding its systemic side effects.

## 4. Conclusion

In this study, CAF-integrated RSV bilosomes were prepared (CRB). It combines the effect of both CAF as a target and substrate to adenosine A1 receptors and RSV in managing obesity and enhancing fat loss. Results showed an approximately 1.5-fold increase in RSV and CAF deposition from CRB compared to RB and CB. This increase in the deposited drugs in fat tissue resulted from CAF targeting effect on fat cells. Also, the amount deposited in the skin acts as a depot for sustained drug release.

After 4 weeks of treatment of obesity-induced rats, rats treated with CRB gel formulations showed a significant reduction in abdominal circumference, loss of body weight, and browning of WAT. Histological examination of the excised full-thickness skin showed a decrease in the subcutaneous fat layer thickness and a decrease in the size of connective tissue-embedded fat cells. This confirms the high ability of prepared caffeinated-resveratrol nanobilosomes (CRB) in managing obesity and cellulite. Kidney histological examination of rats treated with RB reflected a slight systemic effect of RSV from RB. This indicated less targeting effect on adipose tissue compared to CB and CRB. This proves that CAF in CRB helps in the targeting and deposition of RSV in adipose tissue and assists its local acting effect for managing obesity and cellulite while avoiding its systemic side effects.

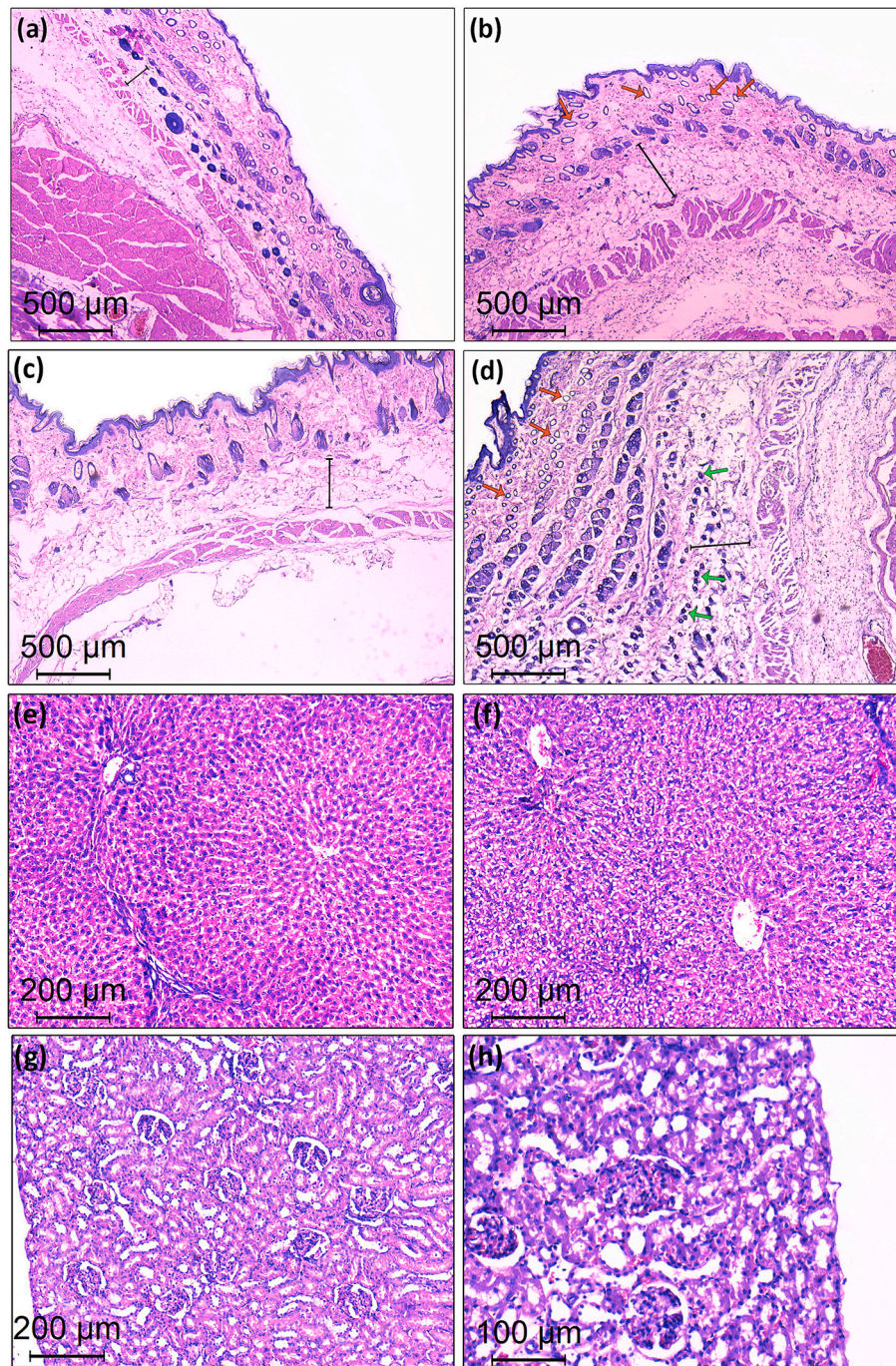


**Fig. 5.** Histological examination for full thickness skin (a-d) and isolated liver and kidney (e-h) stained with H&E stain using optical light microscope. The figure represents skin of: (a) normal rats, (b) obese rats, (c) rats treated with CAF-RSV-gel, (d) rats treated with CRB gel (CAF-RSV bilosomal gel), (e) liver section from normal rats, (f) liver section from rats treated with CRB gel. (g) Kidney section from normal rats and (h) kidney section from rats treated with resveratrol bilosomal gel (RB gel) with magnification X100 that are showing cytoplasmic vacuolation. (O) represent the thickness of subcutaneous fats, (□) represent adipose tissue imbedded in connective tissue that reflect the formation of cellulite, and (○) represent the presence of drug-loaded bilosomal formulations deposited in adipose tissue. Parts of this figure were reproduced from (Khalil et al., 2022) with License number 5604821115777.

### Funding

This research was funded by the Deanship of Scientific Research at King Khalid University through large group Research Project under grant number RGP2/55/44.

### Institutional review board statement

The study was conducted by the protocol approved by the Animal

Care & Use Committee of the Faculty of Pharmacy, Alexandria university (Approval number: 0620192138) on February 9th, 2019.

### Informed consent statement

Not applicable.

## CRedit authorship contribution statement

**Lobna M. Khalil:** Writing – original draft, Methodology, Formal analysis, Data curation. **Wessam M. El-Refaie:** Writing – review & editing, Methodology, Conceptualization. **Yosra S.R. Elnaggar:** Writing – review & editing, Methodology, Formal analysis, Data curation, Conceptualization. **Hamdy Abdelkader:** Writing – review & editing, Methodology, Investigation, Funding acquisition, Data curation. **Adel Al Fateaseh:** Writing – review & editing, Methodology, Funding acquisition. **Ossama Y. Abdallah:** Writing – review & editing, Validation, Supervision, Data curation, Conceptualization.

## Declaration of competing interest

The authors declare no conflict of interest.

## Data availability

Data will be made available on request.

## Acknowledgments

The authors extend their appreciation to the Deanship of Scientific Research at King Khalid University for funding this work through large group Research Project under grant number RGP2/55/44.

The investigation and interpretation of histological data was gratefully conducted by Dr. Maram M. Allam, Lecturer of Pathology, Pathology Department, Faculty of Medicine, Alexandria University. We would like to acknowledge the copyright center of Elsevier for providing copyright agreements with license number 5604821115777

## Appendix A. Supplementary data

Supplementary data to this article can be found online at <https://doi.org/10.1016/j.ijpx.2024.100236>.

## References

- Aburahma, M., 2016. Bile salts-containing vesicles: promising pharmaceutical carriers for oral delivery of poorly water-soluble drugs and peptide/protein-based therapeutics or vaccines. *Drug Delivery* 23 (6), 1847–1867.
- Ahad, A., Raish, A., Al-Jenoobi, A., Al-Mohizea, A., 2018. Eprosartan mesylate loaded bilosomes as potential nano-carriers against diabetic nephropathy in streptozotocin-induced diabetic rats. *Eur. J. Pharm. Sci.* 111, 409–417.
- Algul, D., Duman, S., Ozdemir, E., Acar, Yener, G., 2018. Preformulation, Characterization, and In Vitro Release Studies of Caffeine-Loaded Solid Lipid Nanoparticles. *J. Cosmet. Sci.* 69, 165–173.
- Azizi, M., E. F., Partoazar A., Ejtemaei Mehr S, Amani A., 2017. Efficacy of nano- and microemulsion-based topical gels in delivery of ibuprofen: an in vivo study. *J. Microencapsul.* 34 (2), 195–202.
- Benech-Kieffer, F., Wegrich, P., Schaefer, H., 1997. Transepidermal water loss as an integrity test for skin barrier function in vitro: assay standardization. *Perspectives in Percutaneous Penetration* 5, 56.
- Bézin, N., Arab-Tehrany, E., Loing, E., Bézin, C., 2017. Skin delivery of hydrophilic molecules from liposomes and polysaccharide-coated liposomes. *Int. J. Cosmet. Sci.* 39 (4), 435–441.
- Calle, E.E., Rodriguez, C., Walker-Thurmond, K., Thun, M.J., 2003. Overweight, Obesity, and Mortality from Cancer in a Prospectively Studied Cohort of US adults. *N. Engl. J. Med.* 348 (17), 1625–1638.
- Carrageta, D.F., Dias, T.R., Alves, M.G., Oliveira, P.F., Monteiro, M.P., Silva, B.M., 2018. Anti-obesity potential of natural methylxanthines. *J. Funct. Foods* 43, 84–94.
- Carreiro, A.L., Buhman, K.K., 2019. Chapter 3 - Absorption of Dietary Fat and its Metabolism in Enterocytes. *Academic Press, The Molecular Nutrition of Fats*. V. B. Patel, pp. 33–48.
- Crowell, J.A., Korytko, P.J., Morrissey, R.L., Booth, T.D., Levine, B.S., 2004. Resveratrol-associated renal toxicity. *Toxicol. Sci.* 82 (2), 614–619.
- Davidov-Pardo, G., McClements, D.J., 2014. Resveratrol encapsulation: Designing delivery systems to overcome solubility, stability and bioavailability issues. *Trends Food Sci. Technol.* 38 (2), 88–103.
- Doris Hexsel, M.S., Mazzuco, Rosemari, Dal'Forno, Taciana, Zechmeister, Debora, 2003. Phosphatidylcholine in the treatment of localized fat. *J. Drugs Dermatol.* 2 (5), 511–518.
- El-Mezayen, N.S., El-Hadidy, W.F., El-Refaie, W.M., Shalaby, T.I., Khattab, M.M., El-Khatib, A.S., 2018. Oral vitamin-A-coupled valsartan nanomedicine: High hepatic stellate cell receptors accessibility and prolonged enterohepatic residence. *J. Control. Release* 283, 32–44.
- Elnaggar, Y.S.R., El-Massik, M.A., Abdallah, O.Y., 2011a. Fabrication, appraisal, and transdermal permeation of sildenafil citrate-loaded nanostructured lipid carriers versus solid lipid nanoparticles. *Int. J. Nanomedicine* 6, 3195–3205.
- Elnaggar, Y.S.R., El-Massik, M.A., Abdallah, O.Y., 2011b. Sildenafil citrate nanoemulsion vs. self-nanoemulsifying delivery systems: rational development and transdermal permeation. *Int. J. Nanotechnol.* 8 (8–9), 749–763.
- Field, A.E., Coakley, E.H., Must, A., Spadano, J.L., Laird, N., Dietz, W.H., Rimm, E., Colditz, G.A., 2001. Impact of Overweight on the risk of developing Common Chronic Diseases during a 10-year period. *JAMA Intern. Med.* 161 (13), 1581–1586.
- Frankel, E.N., German, J.B., Kinsella, J.E., Parks, E., Kanner, J., 1993. Inhibition of oxidation of human low-density lipoprotein by phenolic substances in red wine. *Lancet* 341 (8843), 454–457.
- Fredholm, B.B., Persson, C.G.A., 1982. Xanthine derivatives as adenosine receptor antagonists. *Eur. J. Pharmacol.* 81 (4), 673–676.
- Gerbaix, M., Metz, L., Ringot, E., Courteix, D., 2010. Visceral fat mass determination in rodent: Validation of dual-energy X-ray absorptiometry and anthropometric techniques in fat and lean rats. *Lipids Health Dis.* 9, 140.
- Giovanni Salti, I.G., Tantussi, Franca, Bovani, Bruno, Lotti, Torello, 2008. Phosphatidylcholine and Sodium Deoxycholate in the Treatment of Localized Fat: A Double-blind, Randomized Study. *Dermatol. Surg.* 34 (1), 60–66.
- Gnad, T., Scheibler, S., von Kügelgen, I., Scheele, C., Kilić, A., Glöde, A., Hoffmann, L.S., Reverte-Salisa, L., Horn, P., Mutlu, S., El-Tayeb, A., Kranz, M., Deuther-Conrad, W., Brust, P., Lidell, M.E., Betz, M.J., Enerbäck, S., Schrader, J., Yegutkin, G.G., Müller, C.E., Pfeifer, A., 2014. Adenosine activates brown adipose tissue and recruits beige adipocytes via A2A receptors. *Nature* 516 (7531), 395–399.
- Gunasekaran, S., Sankari, G., Ponnusamy, S., 2005. Vibrational spectral investigation on xanthine and its derivatives—theophylline, caffeine and theobromine. *Spectrochim. Acta A Mol. Biomol. Spectrosc.* 61 (1), 117–127.
- Hamishehkar, H., Shokri, J., Fallahi, S., Jahangiri, A., Ghanbarzadeh, S., Kouhsoltani, M., 2015. Histopathological evaluation of caffeine-loaded solid lipid nanoparticles in efficient treatment of cellulite. *Drug Dev. Ind. Pharm.* 41 (10), 1640–1646.
- Herman, A., Herman, A.P., 2013. Caffeine's Mechanisms of Action and its Cosmetic Use. *Skin Pharmacol. Physiol.* 26 (1), 8–14.
- Hexsel, D.O.C., Zechmeister do Prado, D., 2005. Botanical extracts used in the treatment of cellulite. *Dermatol. Surg.* 31 (s1), 866–873.
- Ihedioha, J.I., Noel-Uneke, O.A., Ihedioha, T.E., 2013. Reference values for the serum lipid profile of albino rats (*Rattus norvegicus*) of varied ages and sexes. *Comp. Clin. Pathol.* 22 (1), 93–99.
- Isailović, B.D., Kostić, I.T., Zvonar, A., Dordević, V.B., Gašperlin, M., Nedović, V.A., Bugarski, B.M., 2013. Resveratrol loaded liposomes produced by different techniques. *Innovative Food Sci. Emerg. Technol.* 19, 181–189.
- Jadeja, R.N., Thounaojam, M.C., Ramani, U.V., Devkar, R.V., Ramachandran, A.V., 2011. Anti-obesity potential of Clerodendron glandulosum. Coleb leaf aqueous extract. *J. Ethnopharmacol.* 135 (2), 338–343.
- Khalil, L.M., Abdallah, O.Y., Elnaggar, Y.S.R., El-Refaie, W.M., 2022. Novel dermal nanobilosomes with promising browning effect of adipose tissue for management of obesity. *Journal of Drug Delivery Science and Technology* 74, 103522.
- Kim, J.Y., Song, J.Y., Lee, E.J., Park, S.K., 2003. Rheological properties and microstructures of Carbopol gel network system. *Colloid Polym. Sci.* 281 (7), 614–623.
- Knowler, W.C., Barrett-Connor, S.E., Fowler, R.F., Hamman, Lachin, J.M., Walker, E.A., Nathan, D.M., G. Diabetes Prevention Program Research, 2002. Reduction in the incidence of type 2 diabetes with lifestyle intervention or metformin. *N. Engl. J. Med.* 346 (6), 393–403.
- Komeil, I.A., El-Refaie, W.M., Gowayed, M.A., El-Ganainy, S.O., El Achy, S.N., Huttunen, K.M., Abdallah, O.Y., 2021. Oral genistein-loaded phytosomes with enhanced hepatic uptake, residence and improved therapeutic efficacy against hepatocellular carcinoma. *Int. J. Pharm.* 601, 120564.
- Kotańska, M., Dziubina, A., Szafarz, M., Mika, K., Reguła, K., Bednarski, M., Zygmunt, M., Drabczyńska, A., Sapa, J., Kieć-Kononowicz, K., 2020. KD-64—A new selective A2A adenosine receptor antagonist has anti-inflammatory activity but contrary to the non-selective antagonist—Caffeine does not reduce diet-induced obesity in mice. *PLoS One* 15 (6), e0229806.
- Latosinska, J.N., Latosinska, M., Olejniczak, G.A., 2014. Topology of the Interactions Pattern in Pharmaceutically Relevant Polymorphs of Methylxanthines (Caffeine, Theobromine, and Theophylline): combined Experimental (1 H–14N Nuclear Quadrupole double Resonance) and Computational (DFT and Hirshfeld-based) Study. *J. Chem. Inf. Model.* 54, 2570–2584.
- Liu, D.-Z., Chen, W.-Y., Tasi, L.-M., Yang, S.-P., 2000. Microcalorimetric and shear studies on the effects of cholesterol on the physical stability of lipid vesicles. *Colloids Surf. A Physicochem. Eng. Asp.* 172 (1), 57–67.
- Luebberding, S., Krueger, N., Sadick, N.S., 2015. Cellulite: an Evidence-based Review. *Am. J. Clin. Dermatol.* 16 (4), 243–256.
- Mabrouk, A.A., Tadros, M.I., El-Refaie, W.M., 2021. Improving the efficacy of Cyclooxygenase-2 inhibitors in the management of oral cancer: Insights into the implementation of nanotechnology and mucoadhesion. *Journal of Drug Delivery Science and Technology* 61, 102240.
- Marjukka Suhonen, T., Bouwstra, J.A., Urtti, A., 1999. Chemical enhancement of percutaneous absorption in relation to stratum corneum structural alterations. *J. Control. Release* 59 (2), 149–161.
- Mohsen, A.M., Asfour, M.H., Salama, A.A.A., 2017. Improved hepatoprotective activity of silymarin via encapsulation in the novel vesicular nanosystem bilosomes. *Drug Dev. Ind. Pharm.* 43 (12), 2043–2054.

- Muzzarelli, R.A.A., Orlandini, F., Pacetti, D., Boselli, E., Frega, N.G., Tosi, G., Muzzarelli, C., 2006. Chitosan taurocholate capacity to bind lipids and to undergo enzymatic hydrolysis: an in vitro model. *Carbohydr. Polym.* 66 (3), 363–371.
- Negi, P., Aggarwal, M., Sharma, G., Rathore, C., Sharma, G., Singh, B., Katare, O.P., 2017. Niosome-based hydrogel of resveratrol for topical applications: an effective therapy for pain related disorder(s). *Biomed. Pharmacother.* 88, 480–487.
- Novelli, E.L.B., Diniz, Y.S., Galhardi, C., Ebaid, G., Mani, F., Fernandes, A., Cicogna, A., Filho, J., 2007. Anthropometrical parameters and markers of obesity in rats. *Lab. Anim.* 41, 111–119.
- Omi, T., Sato, S., Kawana, S., 2013. Ultrastructural assessment of cellulite morphology: clues to a therapeutic strategy? *Laser therapy* 22(2), 131–136.
- Organization, W. H., 2020. **Obesity and overweight.** March 3rd. from. <https://www.who.int/news-room/fact-sheets/detail/obesity-and-overweight>.
- Raza, K., Singh, B., Lohan, S., Sharma, G., Negi, P., Yachha, Y., Katare, O.P., 2013. Nanolipoidal carriers of tretinoin with enhanced percutaneous absorption, photostability, biocompatibility and anti-psoriatic activity. *Int. J. Pharm.* 456 (1), 65–72.
- SCHWABE, T. T. A. U., 1980. Adenosine Receptors in Fat Cells. *Mol. Pharmacol.* 19, 228–235.
- Shalaby, T.I., El-Refaie, W.M., Shams El-Din, R.S., Hassanein, S.A., 2020. Smart Ultrasound-Triggered Doxorubicin-Loaded Nanoliposomes with improved Therapeutic Response: A Comparative Study. *J. Pharm. Sci.* 109 (8), 2567–2576.
- Siques, P., Brito, J., Naveas, N., Pulido, R., De la Cruz, J.J., Mamani, M., León-Velarde, F., 2014. Plasma and liver lipid profiles in rats exposed to chronic hypobaric hypoxia: changes in metabolic pathways. *High Alt. Med. Biol.* 15 (3), 388–395.
- Teaima, M.H., Abdelhalim, S.A., El-Nabarawi, M.A., Attia, D.A., Helal, D.A., 2018. Non-ionic surfactant based vesicular drug delivery system for topical delivery of caffeine for treatment of cellulite: design, formulation, characterization, histological anti-cellulite activity, and pharmacokinetic evaluation. *Drug Dev. Ind. Pharm.* 44 (1), 158–171.
- Trites, M.J., Clugston, R.D., 2019. The role of adipose triglyceride lipase in lipid and glucose homeostasis: lessons from transgenic mice. *Lipids Health Dis.* 18 (1), 204.
- Vittorio Bertacche, N.L., Nava, Donatella, Pini, Elena, Sinico, Chiara, 2006. Host-Guest Interaction Study of Resveratrol with Natural and Modified Cyclodextrins. *J. Incl. Phenom. Macrocycl. Chem.* 55, 279–287.
- Wang, S., Liang, X., Yang, Q., Fu, X., Rogers, C.J., Zhu, M., Rodgers, B.D., Jiang, Q., Dodson, M.V., Du, M., 2015. Resveratrol induces brown-like adipocyte formation in white fat through activation of AMP-activated protein kinase (AMPK)  $\alpha$ 1. *Int. J. Obes.* 39 (6), 967–976.
- Yang, L., Xu, Y., Su, Y., Wu, J., Zhao, K., Chen, J.E., Wang, M., 2005. FT-IR spectroscopic study on the variations of molecular structures of some carboxyl acids induced by free electron laser. *Spectrochim. Acta A Mol. Biomol. Spectrosc.* 62 (4), 1209–1215.